

Article

GIS Modeling to Climate Change Adaptation by Reducing Evaporation in Water Reservoirs: Smart Location Technique of Minimal Evaporation Reservoirs (GIS-MER)

Alfredo Fernández-Enríquez^{1,2}, María Luisa Pérez-Cayeiro³ and Giorgio Anfuso^{4,*} 

¹ Departamento Historia, Geografía y Filosofía, Facultad de Filosofía y Letras, Universidad de Cádiz, Av. Gomez Ulla s/n, 11003 Cádiz, Cádiz, Spain

² Research Institute for Sustainable Social Development (INDESS), Av. Universidad 4, 11405 Jerez de la Frontera, Cádiz, Spain

³ Departamento Historia, Geografía y Filosofía, Facultad de Ciencias del Mar y Ambientales, Universidad de Cádiz, Polígono Río San Pedro s/n, 11510 Puerto Real, Cádiz, Spain

⁴ Departamento de Ciencias de la Tierra, Facultad de Ciencias del Mar y Ambientales, Universidad de Cádiz, Polígono Río San Pedro s/n, 11510 Puerto Real, Cádiz, Spain

* Correspondence: giorgio.anfuso@uca.es

Abstract: The ideal emplacement of reservoirs has been traditionally determined by means of GIS tools to prospect large areas applying criteria related to rainfall, substrate impermeability or economic and social viability. More recently, geomorphometric characteristics have been added to determine more suitable locations for dams and reservoirs depending on their dimensions. This study presents a fully automatized ArcGIS Pro model, suitable for working with several digital elevation model resolutions and for evaluating best potential reservoir locations to reduce evaporation losses. Here, a smart location strategy to preserve water resources is used based on the premise that the higher the ratio of water stored to water surface area of the reservoir, the lower the water evaporation. The model was tested in two dissimilar basins in the province of Cadiz (SW Spain) and the results are compared with the nearby existing reservoirs. The methodology presented in this paper allows selecting the most suitable sites where it is possible to build a reservoir with a water surface smaller than other reservoirs but also able to hold an equal or greater volume of water; this also allows reducing the area occupied by the reservoir. As an example, in the first study case presented in this paper, a new reservoir could store 30.7 m³/m² versus the current 9 m³/m² stored in the nearby existing reservoir. This may reduce the flooded area from 25.4 to just 6.7 km².

Keywords: ArcGIS Pro; drainage basin; evaporation; reservoir; volume/area ratio



Citation: Fernández-Enríquez, A.; Pérez-Cayeiro, M.L.; Anfuso, G. GIS Modeling to Climate Change Adaptation by Reducing Evaporation in Water Reservoirs: Smart Location Technique of Minimal Evaporation Reservoirs (GIS-MER). *Sustainability* **2022**, *14*, 13822. <https://doi.org/10.3390/su142113822>

Academic Editor: Luca Salvati

Received: 8 August 2022

Accepted: 18 October 2022

Published: 25 October 2022

Publisher's Note: MDPI stays neutral with regard to jurisdictional claims in published maps and institutional affiliations.



Copyright: © 2022 by the authors. Licensee MDPI, Basel, Switzerland. This article is an open access article distributed under the terms and conditions of the Creative Commons Attribution (CC BY) license (<https://creativecommons.org/licenses/by/4.0/>).

1. Introduction: Smart Location for Reservoirs

The selection of the optimum location for reservoirs is a key aspect in the evaluation of the long-term performance of these strategic infrastructures and this issue has been gaining importance considering future climate change scenarios [1,2] and the increasing demand for hydroelectric energy [3].

Despite efforts to mitigate climate change effects at a global scale are absolutely necessary [4], in a local scale is also useful to promote climate-friendly agro-ecosystems to cope with higher temperatures and changes in water availability when facing climate shocks [1].

Multiple selection procedures have been implemented to take into account each parameter involved, with particular emphasis on four basic aspects: (i) topography and dimensions of the catchment area; (ii) morphology of the river valley; (iii) geological and geotechnical conditioning factors, and (iv) climate, tied to river flow characteristics and seasonal variability. The latter aspects are indeed of critical relevance and strongly control water quality and, therefore, its potential use, e.g., for human consumption or irrigation [5].

It is estimated that 50% of water for irrigation does not reach its destination, with losses caused by leaks in the network or evaporation in the irrigation channels [4]. However, climate characteristics must also be taken into account, as this can drastically reduce water reserves. In Spain, it is estimated that every year, 8% of the water stored in irrigation reservoirs is lost due to evaporation processes as observed in other Mediterranean countries [6]. In the Pyrenees, a lower evaporation rate of 6% is recorded annually because of the altitude at which the reservoirs are located [7].

In Queensland (Australia), it is estimated that evaporation in irrigation ponds can be as high as 40% [8]. In 2004, evaporation resulted in a loss of 41% and 60% of annual water volume available for human consumption in Lake Superior and Lake Tahoe (USA), respectively [9]. A useful reference for estimating economic losses caused by heavy evaporation losses in a Mediterranean climate is the Alqueva reservoir in Portugal, where every 10 mm of evaporation causes an annual loss of 1.1 million euros [10].

To preserve water resources, the American Meteorological Society is promoting a strategy of conservation at source (CaS) that includes smart location techniques, which are strongly focused on the depth of the reservoir and on water surface extension as two of the key physical properties for reducing evaporation, in addition to others more closely related to meteorological characteristics [9].

Therefore, evaporation can be reduced a priori by selecting sound locations, i.e., emplacements where it is possible to create reservoirs that can store the largest volumes of water with the smallest water surfaces. This is because low evaporation rates are not only linked to the water surface area exposed to physical vectors such as atmospheric pressure, wind, solar radiation and air temperature, but especially to the reservoir depth. Given that evaporation depends to a great extent on the surface temperature of the water, the increase in depth also leads to a time lag compared to the solar radiation, while an increase in the surface area has very little effect on the annual evolution of the temperature and the evaporation rate [7,9,11].

According to a literature review carried out by Wang et al. [4], the application of GIS tools for the selection of sound reservoir locations is very common. Previous authors consulted 148 highly relevant articles published between 2000 and 2020 and observed that only 10% of them included evaporation in the selection of sound locations and, in general, followed three principal methodologies:

(i) The use of GIS and Remote Sensing. Endless hydrological models have been developed with GIS tools, essentially devoted to the prevention of natural disasters. Presently, very detailed Digital Elevation Models (DEM) are generated using LiDAR (Light Detection and Ranging), which can be used to provide very accurate topographical information [12]. In addition, models usually include a myriad of geospatial information and data obtained via remote sensing and allow the generation of complex systems often involving multiple indices [13] to support decision-makers [14].

(ii) The Multi-criteria Selection, usually based on a sequence of steps. The first step is the selection of large suitable areas [15]. The second step is a weighted overlay process involving different aspects according to specific priority factors [16] such as the typology/function of the required reservoir: the supply of drinking water, irrigation requirements, flood control and hydroelectric generation. Models have been implemented to identify and select areas where terraces can be modeled to conserve water and soil [17]. Recently, the classic AHP (Analytic Hierarchy Process) and TOPSIS (Technique for Order of Preference by Similarity to Ideal Solution) [18] have been combined with fuzzy logic [19,20].

(iii) Deep Learning. Spatial Decision Support Systems (SDSS) are giving rise to intelligent decision-making tools (intelligent Decision Support Systems, iDSS), complementing the multi-criteria analysis with artificial intelligence techniques by means of deep learning techniques [21].

This study proposes a new method (GIS-MER, Minimum Evaporation Reservoirs), based on GIS tools, which allows the determination of the ideal location for a reservoir with a water surface smaller than other reservoirs but also able to hold an equal or greater

volume of water. As an advantage, the method presented here does not need auxiliary information and uses exclusively topographic data (DEM, Digital Elevation Model), to automatically carry out the evaluation of large areas in order to select sound potential sites for the emplacement of reservoirs, i.e., places with low evaporation rates, usually obtained by reducing the surface area exposed to evaporation [8]. To this end an automated procedure was designed to locate potential sites for the emplacement of dams, calculate the parameters of the resulting reservoirs and, finally, to select the site or sites that offer a better volume/surface area ratio, expressed in m^3/m^2 .

Concerning previous studies, Walsh et al. [12] described the North Carolina Reservoir Siting tool (NC-RES) that uses ArcGIS 10.1 to automate the basic evaluation and selection of potentially sound sites for the emplacement of reservoirs. It uses LiDAR terrain models, with resolutions from 20 to 80 feet (6 to 25 m approximately), and Web servers. The tool is suitable for users with no prior training and users only have to specify the object of the study by entering a location point and other simple parameters. This model gives a visual representation of the inundation area and its surface, of the volume of water retained and the catchment area, in addition to data on the administrative borders and soil uses along with the area considered. This model is not able to evaluate large areas to determine the most suitable locations, as the GIS-MER method proposed in this paper does.

The DamSite model [22], based on the use of Python and R scripts, is available for free (upon request), and its purpose is to simplify the studies required for the selection of sites and uses DEM and hydro-climatic data to analyze large areas of terrain ranking the potential sites. The model, tested in two case studies in northern Australia, is able to quickly provide the location and height of the dam, but not its length or the volume and surface area of the reservoir as provided by the GIS-MER.

Wimmer et al. [23] presented an algorithm that identifies contour lines suitable to be closed by a dam, outlining a multitude of polygons that are later analyzed in detail to provide the location of all possible reservoirs. It uses shapefiles with contour lines obtained from a DEM and identifies the upper height of the dam. As a negative aspect, the model does not provide the volume of the potential reservoirs and is not integrated in a GIS project.

Last, the LOCASIN model [24] (Location detection of retention and detention basins) was written in MATLAB and is distributed as an open source user-friendly model. The model works at different scales and can be used to locate small or large reservoirs. In addition to a DEM of the area studied, it needs to include layers obtained from previous hydrological analysis (containing information on flow direction and accumulation, water network and a 70-m buffer) and soil uses. Multi-criteria techniques are used in the decision-making process but it does not have an easy-to-use graphic interface.

2. Study Area

The majority of the province of Cádiz in southwestern Spain, is located within the basins of the Guadalete and Barbate rivers (Figure 1).

The origin of the Guadalete river is in the Grazalema mountain ridge, a Subbaetic limestone massif with a steep, rocky relief. The Barbate river begins in the Sierra del Aljibe, a Penibaetic sandstone forming hills characterized by long and deep gorges (up to 100 m in depth). In both cases valley bottoms are mostly filled up by an impermeable substrate constituted by clays (Figure 2).

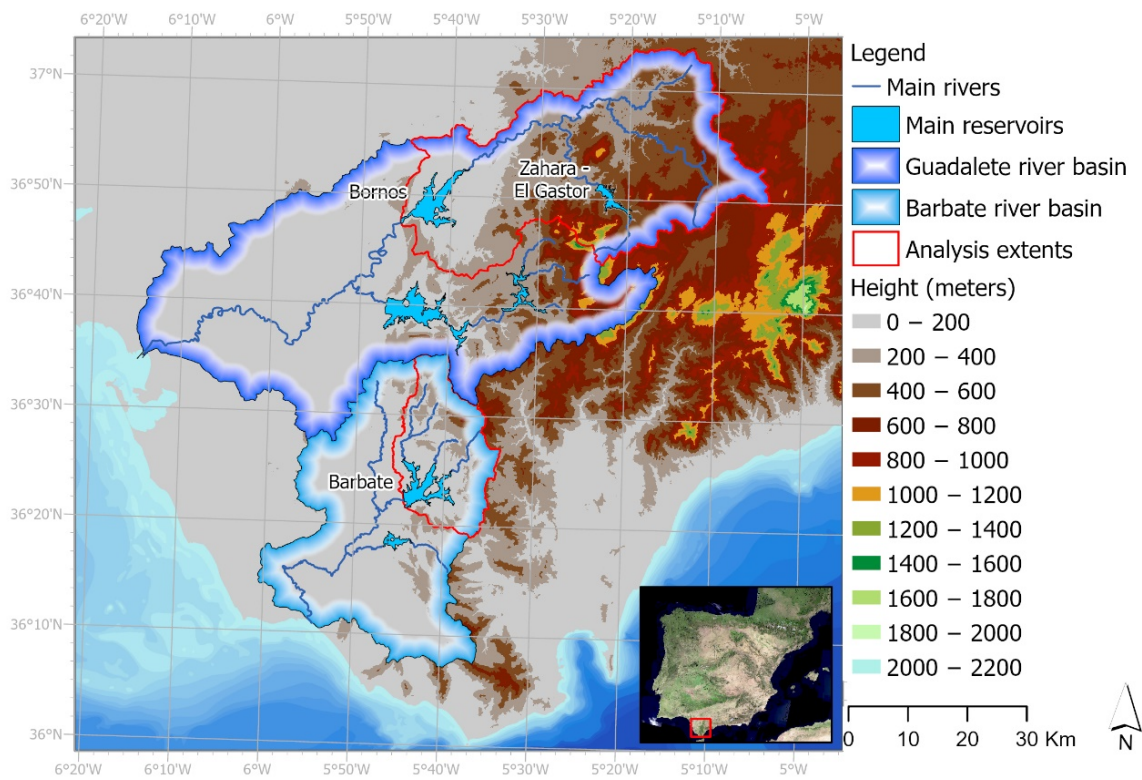


Figure 1. Location of the case studies, modified from *Instituto de Estadística y Cartografía de Andalucía* [25].

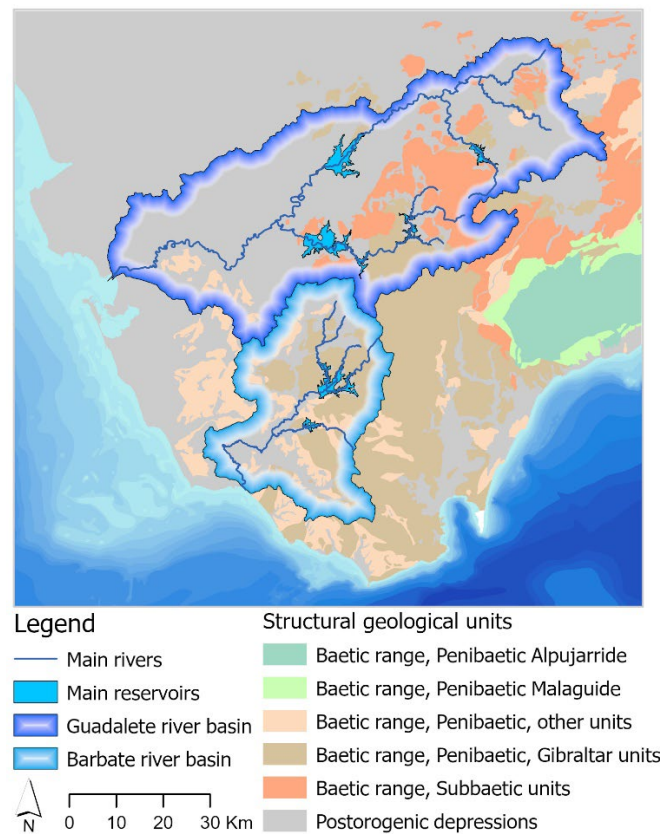


Figure 2. Structural geological units, modified from *Red de Información Ambiental de Andalucía* [26].

The average annual rainfall in both basins ranges from the coastal 500 mm. to over 2000 mm. found in the higher mountains, which has one of the highest precipitation rates in Spain since it creates a barrier perpendicular to the rainy southwesterly winds, coming from the Atlantic Ocean. The influence of the sea also moderates temperatures, with averages between 18 °C in summer on the coast and 8 °C in winter in the mountains, corresponding to a Mediterranean climate, Köppen Csa in the lower altitude and Csb in the higher ones [27].

With regard to the Barbate river basin, the present study only considered the upper section of this basin, where the Barbate reservoir receives water from the homonymous river and three parallel tributaries flowing in gorges up to 100 m in depth.

This reservoir is an ideal case study because it is located on a lowland, which implies high evaporation rates. The small size of this basin favors the use of the DEM 5 by means of a quick analysis and results are easily verified and useful for illustrating the procedure used within the GIS-MER model.

With regard to the Guadalete river basin, its surface is much more extensive; therefore, the study area does not comprise the whole basin, but just the mountainous western part of the basin.

The southern tributary (Figure 1) was not considered because it is almost completely regulated by two major reservoirs. On the other hand, the upper section of the Guadalete basin has large unregulated sections and two major reservoirs (Figure 1 and Table 1). Features of all existing reservoirs considered in this study are presented in Table 1.

Table 1. Main reservoirs in the province of Cádiz [28].

	Barbate	Bornos	Zahara-El Gastor
Surface area of the drainage basin (km ²)	355	1344	129
Crest length (m.)	1359	164	420
Crest height (m.)	42	109	357
Height from the river bed at the dam (m.)	12	45	127
Surface area of the reservoir at maximum normal level (MNL) (hectares)	2540	2341	723
Capacity at MNL (hm ³)	231	215	223
Height of the MNL (m.)	37	104	352

3. Materials and Methods

ArcGIS Pro model builder was used to create a model containing 13 submodels (with further 6 nested), i.e., GIS-MER (Minimum Evaporation Reservoirs). It is sufficient to enter the DEM in a raster format and the maximum desired length for the dam to run the tool: all the available sites in the area will be automatically obtained highlighting the ones that provide the best volume/surface area ratio, in m³/m².

The GIS-MER model uses ArcGIS Pro, rather than open source software or earlier versions of ArcGIS, and is simple to run given that it only requires a DEM (Digital Elevation Model), avoiding the need for complex implementation of SDSS.

The model (Appendix A, Figure A1) systematizes all the necessary operations (mainly hydrological and topographical analysis) in 13 sub-models, with a further six nested, giving a total of 19 sub-models (some of the most relevant are shown in Appendix B, Figures A2–A6). The execution interface used is the Geoprocessing panel (Appendix C, Figure A7), because the use of iterators prevents the export of the model as a Python script to generate a specific interface.

Both Model 5 and Model 10 are already set to run; just few parameters can be adjusted to fit local conditions. Running the model will execute 126 tools consecutively; each one is set to provide the necessary inputs layers for the next step (Figure 3). Besides, 15 iterators ensure the execution of respective submodels and this is accomplished for every value presented in the input layers.

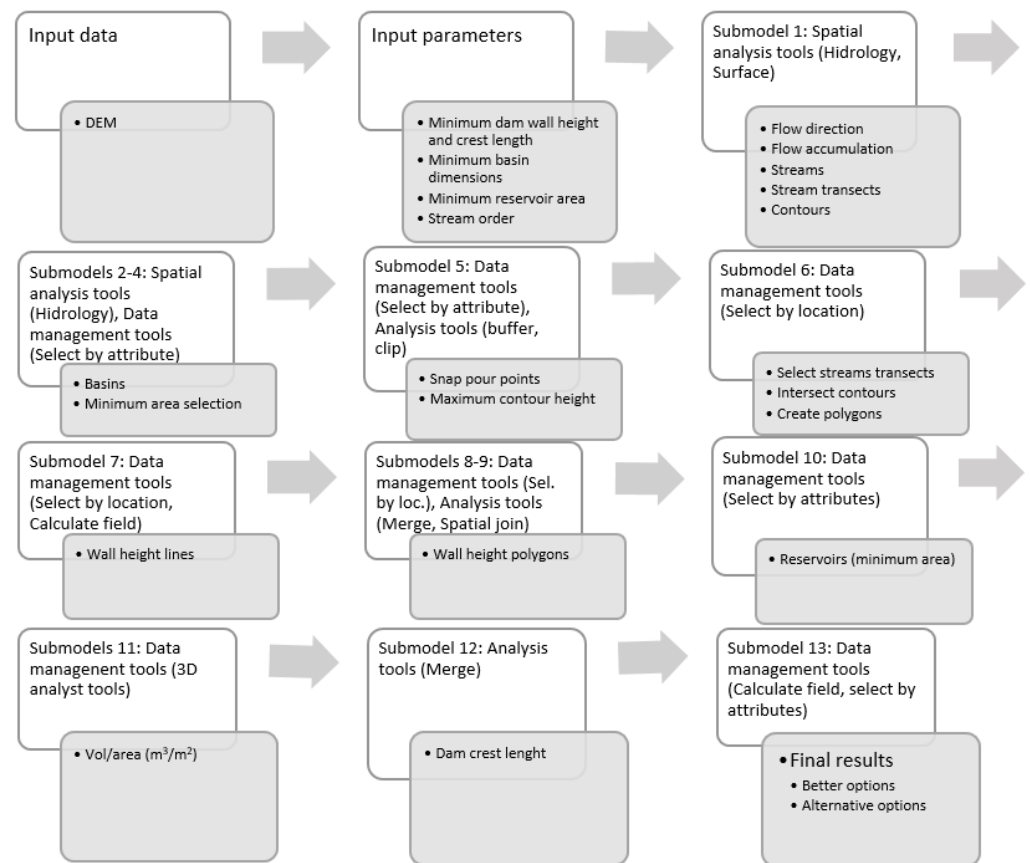


Figure 3. Overview: main tools and outputs for each submodel.

Including 31 tools, submodels 1–4 are intended to: (i) create contours; (ii) to calculate hydrological standards, as flow direction and accumulation, streams, pour points and basins; and (iii) filter the outputs ensuring they fit the parameters previously established, such as streams minimum Strahler order and minimum basin dimensions.

Submodels 5–6 use 30 tools to: (i) intersect snap pour points, streams transect and contours; (ii) select the higher value from contours surrounding each snap pour point and (iii) create polygons to delimitate potential reservoirs.

Submodels 7–10 use 20 tools to: (i) calculate wall height on stream transects lines; (ii) join the coincident polygons and (iii) select those having the minimum desired area.

The final stage involves 44 tools distributed in the submodels 11–13 to: (i) create TINs; (ii) calculate volume and volume/area ratio (in m^3/m^2) and (iii) to measure dam crest lengths for the final set of selected locations, highlighting the most suitable one.

The folder GIS-MER.zip, available in the Mendeley Data repository, provides an ArcGIS Pro project containing the DEMs and two copies of the model, fully implemented and ready to be run when placed in drive C ($C:\text{GIS_MER}$), taking into account the specific characteristics of the two case studies.

The only information that is strictly necessary to carry out calculations is a DEM (Digital Elevation Model). It should be noted that, in the DEM, the water surface of the existing reservoirs is shown as the ground height, and the real height of the ground under the water reservoir is unknown. Consequently, in order to be able to compare the characteristics of the potential sites with the presently existing reservoirs, data from official sources are required (volume and surface area of the reservoir, and height and length of the crest dam wall).

Concerning the spatial scales used, DEM 5 and DEM 10 have been selected because both the DEM 20 and SRTM 30 scales were tested and did not allowed to obtain satisfying results in both the two study cases.

The substantial differences in the geomorphological configuration of the upper river sections of the two studied basins, highlights the versatility of the model. The Barbate reservoir basin, which is smaller, allowed the use of a DEM with a resolution of 5 m, whereas in the Guadalete basin, which is much larger, the resolution used was 10 m.

The Model 5 is devoted to the first study case. The model is configured with the DEM 5 and a dam crest whose maximum length reaches 1359 m at the Barbate reservoir dam. Setting this value as a length restriction will ensure to find alternative locations for equal or shorter dams.

In the second case study, the Model 10 is set to work with the DEM10 and a maximum length for the dam crest of 420 m, similar to that of the Zahara-El Gastor reservoir. The other parameters can also be configured to adapt the process to the study area. In these two models the only change is the search distance for the transects in the immediate vicinity of the drainage point, set at 1 m for the DEM 5 and 10 m for the DEM 10. This parameter needs to be adjusted so that differences in the pixel size do not prevent the selection of the most suitable drainage points. The other parameters remain unchanged: minimum and maximum surface area of the projected reservoir, minimum surface area of the catchment area, minimum dimensions of the dam (minimum height from the crest to the river bed, and maximum length of the crest), minimum value for waterways according to the Strahler classification, minimum surface areas (of the reservoir and its catchment area) and name and destination of the output files. By default, those values are set at 30 m for the minimum height of the dam (or maximum reservoir depth), a minimum of 5 km² and a maximum of 50 km² for the surface area of the reservoir (to ensure water surfaces neither small nor excessive), and a minimum of 40 km² for the catchment area, which may provide sufficient capacity of water recollection.

4. Calculation and Results

4.1. Calculation

As previously stated, Models 5 and 10 can be simply executed by opening the Geoprocessing panel and clicking the Run button (Appendix B). In a first step the water network of the area is obtained, to which filters must be applied in order to exclude waterways lower than order 3 (according to Strahler's terminology/definition). Transects are then drawn with the desired length for the dam and are intersected with contour lines surrounding the waterway, i.e., those that would be closed by a dam wall—the one with the highest height value is finally extracted (Figure 4).

Extracted contour lines and the corresponding transects allow the creation of polygons that represent the reservoir surfaces. When such results are filtered by considering the minimum dam height and the minimum areas of the reservoir surface and its catchment area, the viable alternatives are obtained. Calculation of the ratio between water volume and surface area in m³/m² allows selection of the most suitable alternative.

Different alternative options are obtained by the model, allowing the study of different possibilities, e.g., combining several dams of lower height than those initially detected, simply by adjusting the parameters to run the model again. Subsequently, the final models result show the best location for the dam and a polygon that provides the maximum surface area of the corresponding reservoir; included in the table of attributes is the volume, the surface area, the ratio between them (in m³/m²) and the height and length of the dam.

Finally, the results are presented automatically, displaying in labels the selected option parameters to facilitate immediate comparison with the Table 1 data (Figure 5).

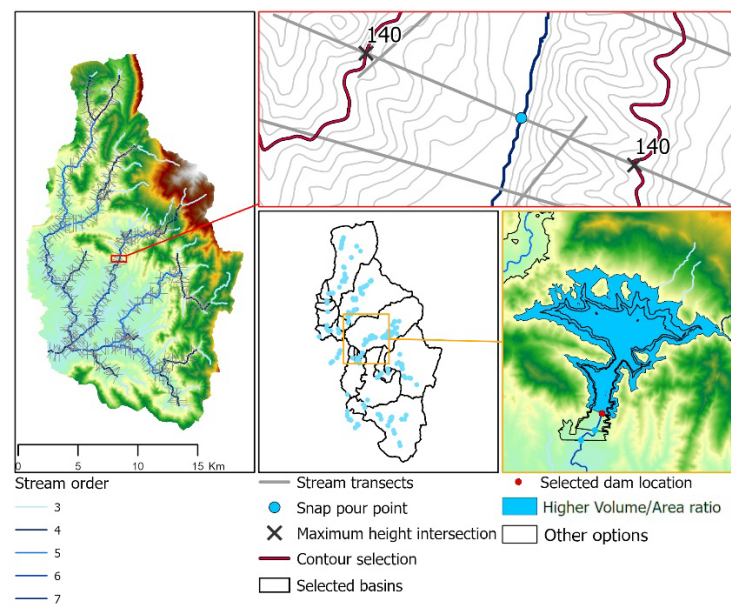


Figure 4. Key steps in the methodology. From left to right and from top to bottom; hydrological calculation of Strahler order 3 waterways and the drawing of transects; intersection with contour lines and identification of the intersecting contour lines surrounding the waterway to extract the highest height value; hydrological calculation of the catchment areas; and final selection of the polygons in accordance with the established requirements.

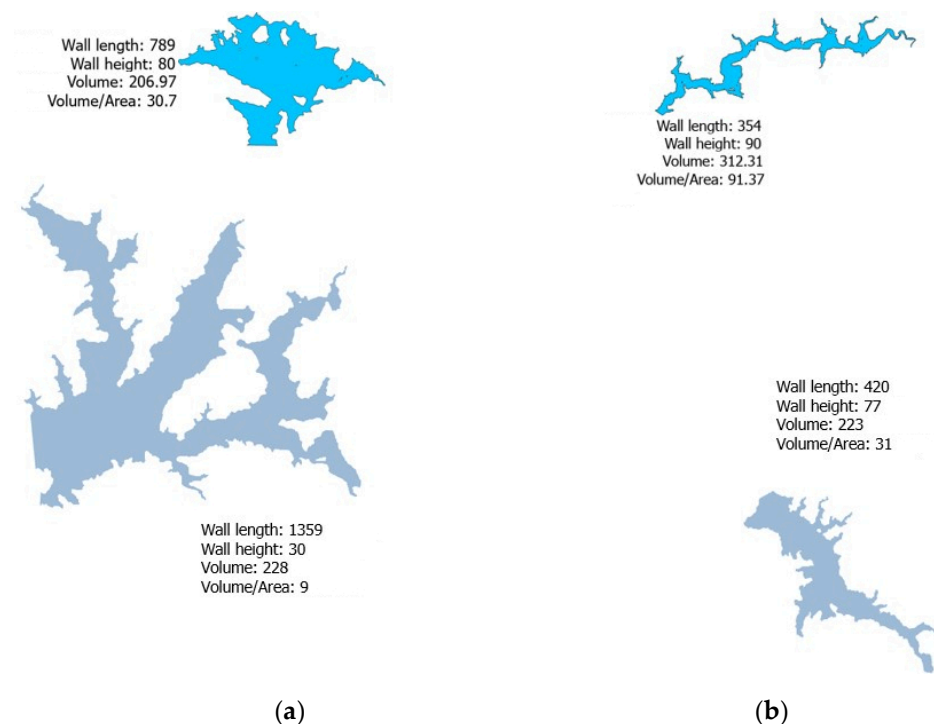


Figure 5. Results shown on the screen after running DEM 5 (a) and DEM 10 (b), compared to the existing reservoirs data (Table 1). Wall length and height in meters; Volume in Hm^3 ; Volume/Area ratio in m^3/m^2 .

4.2. Results

The first case study is the catchment area of the Barbate river reservoir, built in 1992 to bring together the flows from three rivers, one tributary and several streams. Along two of

them, the GIS-MER model identified locations where it is possible to emplace new dams (higher than the existing one) upstream of the current reservoir (Figure 5).

Concerning the river located in the middle of Figure 6, the GIS-MER model identified three possible dams. In the best option, the dam is only 789 m long, i.e., approximately half of the current reservoir (Table 2), and reaches a height of 80 m. The maximum volume of this reservoir would be 208 hm³, not too far from the current 228 hm³ of the Barbate reservoir, and would present a surface area of just 6.88 km², which gives a ratio of 30.91 m³/m², 3.4 times higher than the current one (9 m³/m²). The surface area is just 6.74 km², around a third of the 25.4 km² covered by the Barbate reservoir.

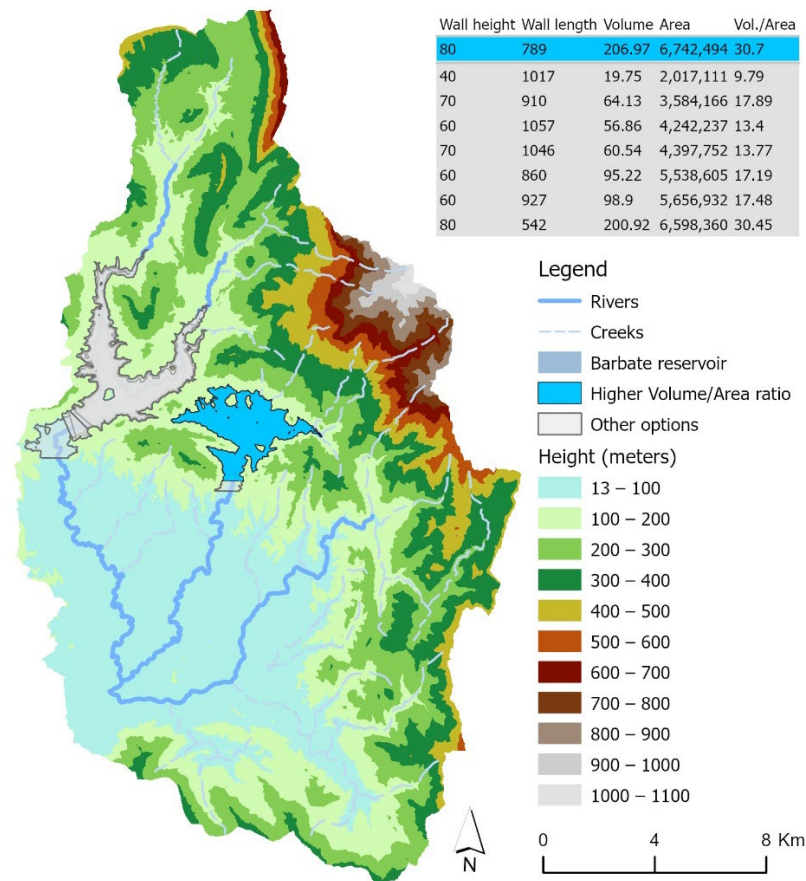


Figure 6. Results of the first case study, in the Barbate river basin (DEM 5). Wall height and length in meters; Area in square meters; Volume in Hm³; Volume/Area ratio in m³/m².

Table 2. Data for the existing Barbate river reservoir [28] and alternative options (Model 5).

	Barbate (Current Reservoir)	Best Option	2nd Option
Wall length (m)	1359	789	927
Wall height (m)	30	80	60
Surface area (km ²)	25.4	6.74	5.77
Volume (hm ³)	231	208.41	99.06
Vol./Surf. (m ³ /m ²)	9	30.91	17.16

In the river located on the left side of Figure 6, the GIS-MER model identified seven possible locations. The most suitable dam wall would be 927 m long and 60 m high, and would create a reservoir with 99.06 hm³, 5.77 km² and 17.16 m³/m². Proposed options have a better volume/surface ratio than the current Barbate reservoir, and they can be combined to build smaller dams and create two or more reservoirs.

In the second case study, focused on the Guadalete basin, the Bornos reservoir is in the mid-section, built in 1961. The Bornos dam wall is 45 m high, located in a narrow gorge reaching a minimum of 164 m in width. On the one hand, this is an ideal location for a dam because such a location allows a shorter crest length; however, on the other hand, flooded terrains are mostly flat, thus it is not possible to increase the water volume stored and reduce the surface area.

The upper section of the Guadalete river, upstream of the Bornos reservoir, only contains the Zahara-El Gastor reservoir, built in 1992 near the source of the Guadalete river with a 420 m-long dam crest, reaching 280 m in height above the river bed. Together with its north bank tributaries, the upper section of the Guadalete river is a good place to examine the possible location of other reservoirs as an alternative to the existing ones.

Once Model 10 has been executed, the map obtained shows that the most advantageous option to reduce evaporation is a location north of the Zahara-El Gastor reservoir. The second option is downstream of the current reservoir (Figure 7).

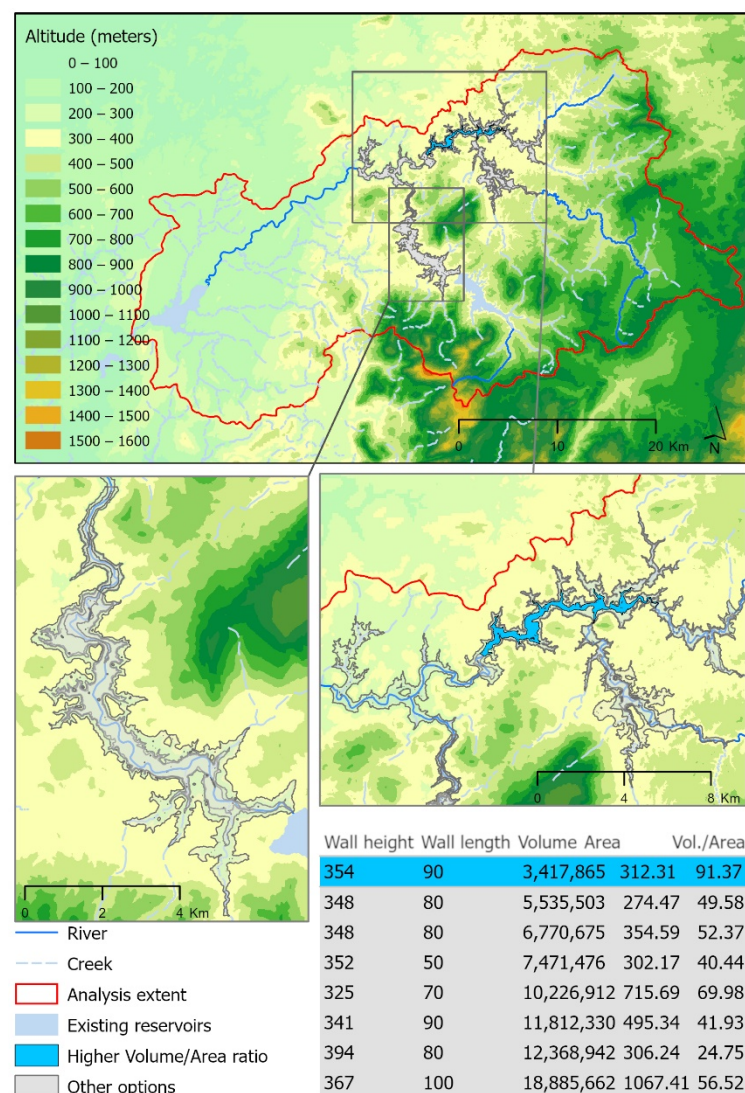


Figure 7. Results of the second case study, in the Guadalete river basin (DEM 10). Wall length and height in meters; Volume in Hm^3 ; Area in square meters; Volume/Area ratio in m^3/m^2 .

The Zahara-El Gastor reservoir was designed for irrigation, and its location provides sufficient height to irrigate agricultural plains 15 km apart.

The comparison between the existing reservoirs and the potential sites (Table 3) shows how the latter have volume/surface area ratios that are evidently advantageous for the

reduction of evaporation. The best alternative option, with $91.37 \text{ m}^3/\text{m}^2$, almost triples the values found in the Zahara-El Gastor reservoir ($31 \text{ m}^3/\text{m}^2$). The 2nd alternative option ($56.52 \text{ m}^3/\text{m}^2$) also considerably exceeds the current existing values.

Table 3. Data for the existing Barbate river reservoir [28] and alternative options (Model 5).

	Bornos	Zahara-El Gastor	1st Option	2nd Option
Wall length (m)	164	420	311	360
Wall height (m)	45	77	70	60
Surface area (km^2)	23.4	7.23	5.75	4.17
Volume (hm^3)	215	223	418	244
Vol./Surf. (m^3/m^2)	9	31	73	59

The best option has a water surface of just 3.41 km^2 , smaller than the existing one in the Zahara-El Gastor reservoir (7.23 km^2). To this small figure for land consumption we have to add the small dam size, just 311 m long, remarkably smaller than the 420 m in the Zahara-El Gastor one, and only larger than the one in Bornos, located in a narrow gorge. The second option is bigger (18.89 km^2), but also has a reduced dam wall length, just 360 m.

5. Discussion

In the introduction session have been presented the most recent and relevant models for reservoir location [12,22–24].

The final selected location for minimum evaporation is not the only difference between the state-of-the-art models and the GIS-MER model. Its novelty relies, as well, in its ability to rapidly evaluate large areas providing both the most suitable locations for the dam, as its height and crest length, and the resulting water storage per unit of surface area. Besides, it is integrated in a GIS project with an easy-to-use graphic interface, making it simple to evaluate alternatives and adjust variables to fit to different scenarios.

As an alternative to Python, R, MatLab and other specific algorithms, GIS-MER is used with ArcGIS Pro, and is sufficient to copy the desired DEM to the geodatabase to run the model in an easy and rapid way.

As previously mentioned, many other location models have been specifically designed to guarantee, for example, the suitability of the substrate and the flow rates, among other technical requirements, and also how procedures may be implemented to prevent social and environmental conflicts. GIS-MER can complement other existing options in ArcGIS Pro, such as those for processing images obtained from remote sensing, multi-criteria evaluation and deep learning, which can be implemented to model the aforementioned requirements and filter those portions of the territory that have impermeable substrates, sufficient flow affluent and suitable water quality for the intended purpose (water supply, electricity generation, etc.) or proximity to lands that require irrigation. It is also compatible with a set of specific tools developed by ESRI for reservoirs, called Dam safety [29], which is used to manage and monitor the routine dam inspection and maintenance tasks.

Different models can be executed in chain to apply successively specific complementary criteria. In addition to the local meteorology, the smart location strategy [9] points to the water depth and the surface area extension of the reservoirs as key physical properties in reducing evaporation. López [7] emphasizes the relevance of reservoir geomorphology and management system as key factors to explain the considerable differences in evaporation between near reservoirs that only show minor differences in meteorological characteristics. The morphology is independent from the management system and the morphological characteristics that can be obtained from the DEM are the only essential data to establish which locations can be used for reservoirs with a higher volume/surface area ratio and, therefore, lower evaporation [7,9,11].

Of course, detailed meteorological aspects must be taken into account once the most suitable locations have been selected. Unfortunately, an efficient automatization of the analysis of meteorological data for the reservoirs is not yet feasible, at least not as easily

as for the topographical data. Evaporation in reservoirs is calculated using a variety of methods based on field data, such as the water temperature collected in situ, or estimated using remote sensing or aerial images, the availability of which greatly varies, or by using the climatological data collected by weather stations located nearby. The diverse methods provide results with large discrepancies, with evaporation losses ranging from 6% to 17% [7]. It is probably more useful to take into account the spatial distribution of the standardized precipitation index (SPI) as additional criteria for evaluating the suitability of small reservoirs [30].

The importance of the water depth of the reservoir in the calculation of the evaporation is most notable in the more advanced methods, which apply energy balance models to irrigation reservoirs. These models take into account dimensions (surface area and reservoir depth) climate data (radiation, wind, humidity, temperature) and use evaporimeter tanks in situ [11]. In the tests carried out by such authors in Cartagena (Spain), it was demonstrated that an increase in depth leads to a time lag between the solar radiation and the water temperature, which in reservoirs deeper than 25 m can be as long as three months. However, Jensen [31] pointed out that the small dimensions of the evaporation tanks and the assumption that they behave in an isothermal manner can lead to an overestimation of the evaporation when results are extrapolated to deep bodies of water, as 70% of the solar radiation is absorbed in the first 5 m of water column. It is more difficult to specify how much radiation penetrates to a greater depth, as it depends on water turbidity.

In summary, evaporation diminishes with smaller surface area and increased depth. When prospecting large areas, data from in situ tanks, analysis and weather stations are limited. Therefore, it is very practical to consider the ratio between depth and surface area using strictly topographical criteria to filter most suitable locations.

Furthermore, it would be relevant in the future to include other criteria related to topography in the GIS-MER model, such as the compactness indicated by Friedrich [9], or the most favorable orientation of the reservoir surface with regard to the surrounding relief, which are determining factors in the incidence of solar radiation throughout the day. For example, within the Guadalete basin study area presented here, the predominant east-west axis in the first (i.e., best) option contrasts with the predominant north-south axis in the 2nd option. A detailed evaluation of the intensity of incident solar radiation and the resulting evaporation might reinforce the first option because it is in a shady zone.

Regarding the ideal depth for prevention of possible harm for aquatic life caused by stratification [32], the development of GIS spatial modelling techniques makes it possible to incorporate variables in the water landscape and identify habitats of macrophytes and other spatial ecological variables that make it possible to improve the management of water resources, from plants to fish, including invasive species [33].

Finally, concerning the spatial scales used, tests have been carried out on the functionality of the model at DEM 20 and SRTM 30 scales, and the results are of very little or no use, as described by Wu et al. [34], who emphasize the dependence on the scale of the DEM with decisive impact on the determination of the slope, the flow trajectory and the basin dimensions, and rules out its usefulness on larger scales, beyond very localized case studies. It has been noticed using different DEM resolutions, which implies strong effects on geomorphological and hydrological calculations: slope estimated values decrease with coarser resolution, whilst upslope estimated values increase as the grid size does. Flow path length and watershed area are also sensitive to changes in the grid size, but do not show any definite trend of bias.

Within this study, the use of more detailed scales has been checked, the DEM 2 multiplies excessively the processing time without improving the definition of the optimum wall dams. In the case studies analyzed with the DEM 5 and the DEM 10, the execution time was approximately 90 min and two hours, respectively.

6. Conclusions

The GIS-MER method, by entering a number of simple parameters, is able to evaluate large areas in order to identify suitable alternatives to locate new dams nearby the existing ones in the area analyzed. The method provides as well as the necessary height for the dam wall, its crest length, the potential flooded area and the water storage volume in order to provide suitable locations with less evaporation rates, greater volumes of water stored and smaller surface areas flooded. It also makes it easier to compare combinations of several small dams as an alternative to large dams, the only requirement being a DEM resolution suitable for the orography complexity of the study area, indeed a key point to ensure accuracy. In the case study cases shown previously, the best results have been obtained with the DEM 5 and the DEM 10.

The proposed workflow might be extended to consider the segmentation of the volumes in each reservoir, as well as to estimate the resulting volumes with dams of different heights, and also to add the compactness of the river bank and the orientation of the reservoir surfaces with regard to the surrounding relief as selection criteria for the most suitable conditions for reducing evaporation. Finally, another possibility lies in combining the GIS-MER method with other location models, for example, those for prior selection of impermeable substrates and sufficient flow rates, or those for evaluating the effects on aquatic life in the potential locations.

Author Contributions: Conceptualization, A.F.-E., M.L.P.-C. and G.A.; methodology, A.F.-E.; software, A.F.-E.; validation, A.F.-E., M.L.P.-C. and G.A.; formal analysis, A.F.-E.; investigation, A.F.-E., M.L.P.-C. and G.A.; resources, M.L.P.-C. and G.A.; data curation, A.F.-E.; writing—original draft preparation, A.F.-E., M.L.P.-C. and G.A.; writing—review and editing, A.F.-E., M.L.P.-C. and G.A.; visualization, A.F.-E., M.L.P.-C. and G.A.; supervision, M.L.P.-C. and G.A.; project administration, A.F.-E., M.L.P.-C. and G.A.; funding acquisition, M.L.P.-C. and G.A. All authors have read and agreed to the published version of the manuscript.

Funding: This publication and research has been partially granted by INDESS (Research Institute for Sustainable Social Development), Universidad de Cádiz, Spain.

Institutional Review Board Statement: Not applicable.

Informed Consent Statement: Not applicable.

Data Availability Statement: GIS_MER.zip available at Mendeley Data Repository: Fernández Enríquez, Alfredo (2022), "GIS_MER", Mendeley Data, V1, doi: 10.17632/nj26vsx2xc.1.

Acknowledgments: This is a contribution to AGUAs21 Research Project (sol201800107890), supported by Regional Department of Economy, Knowledge, Enterprise and University of the Government of Andalusia and European Regional Development Fund (ERDF) and a contribution to the PAI Andalusia Research Group RNM-328.

Conflicts of Interest: The authors declare no conflict of interest.

Appendix A

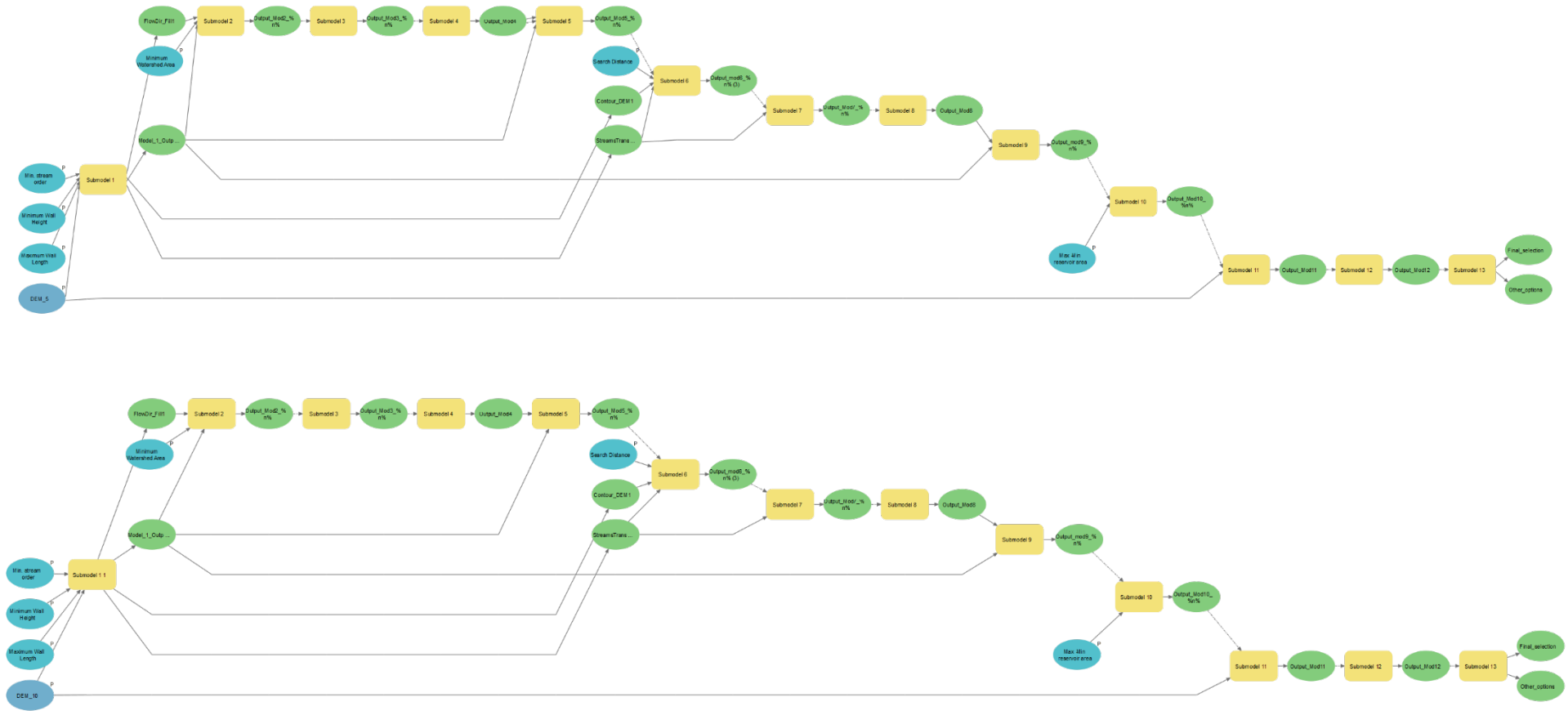


Figure A1. GIS-MER Model 5 and Model 10.

Appendix B

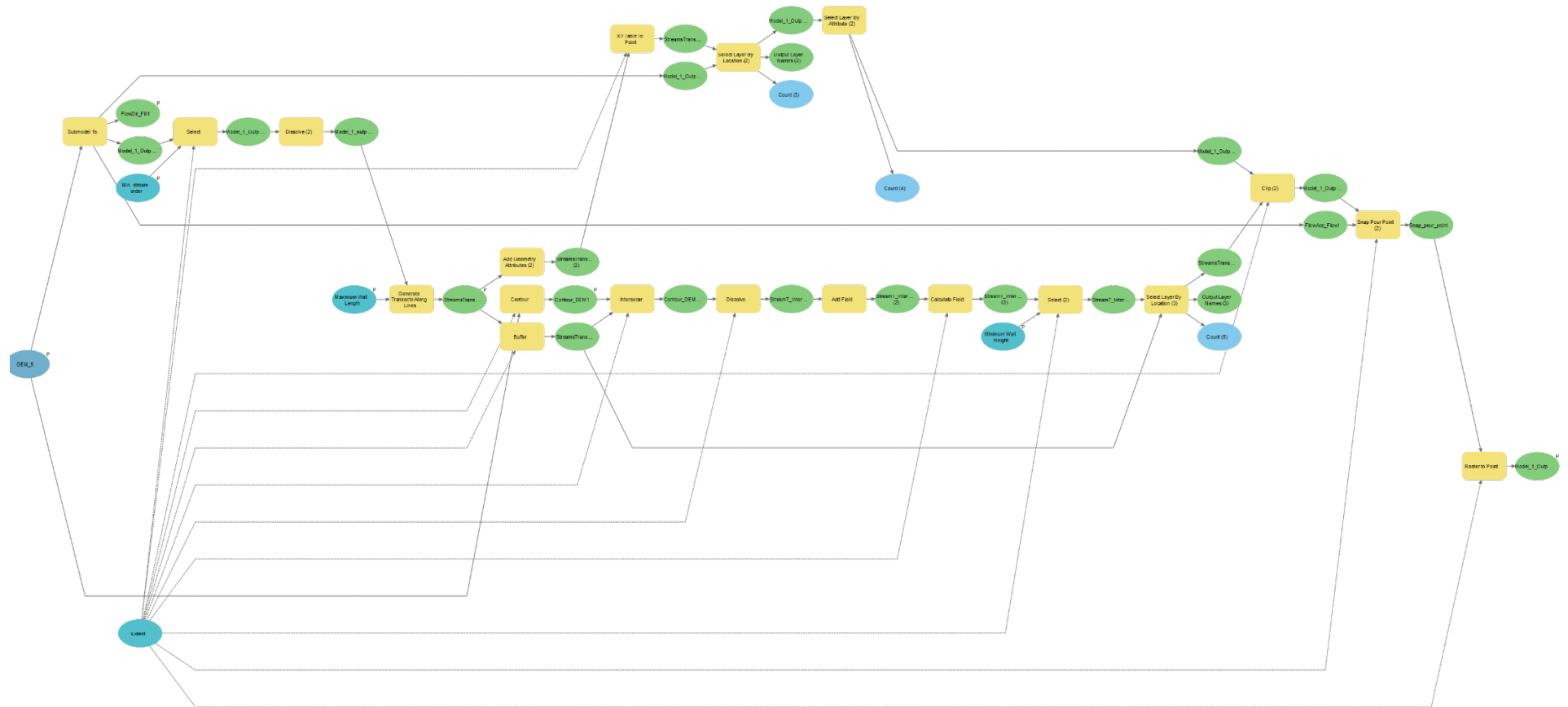


Figure A2. GIS-MER submodel 1 (hydrologic tools).

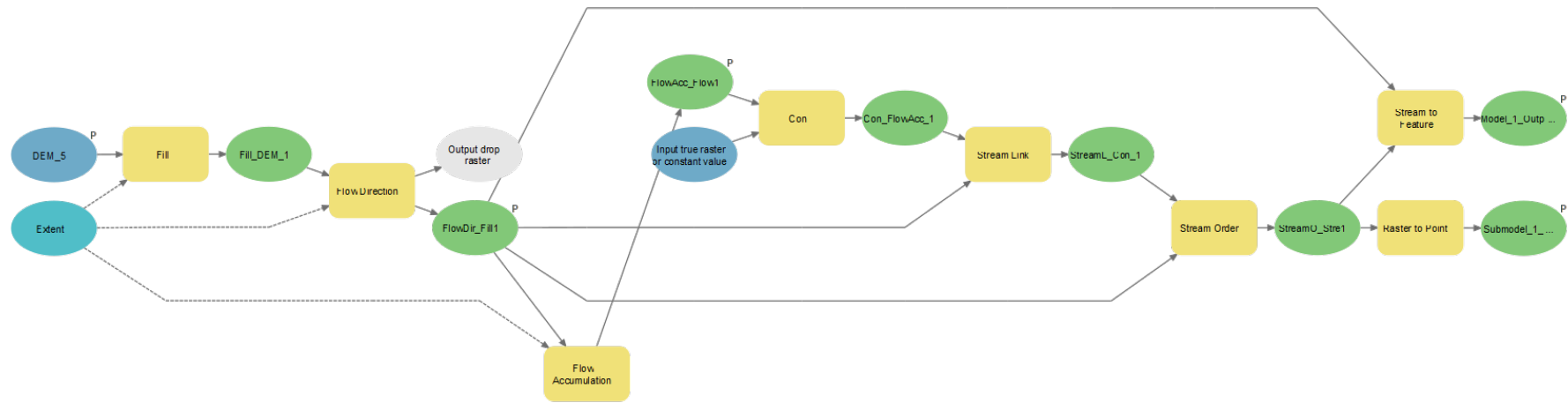


Figure A3. GIS-MER submodel 1b (hidrologic tools).

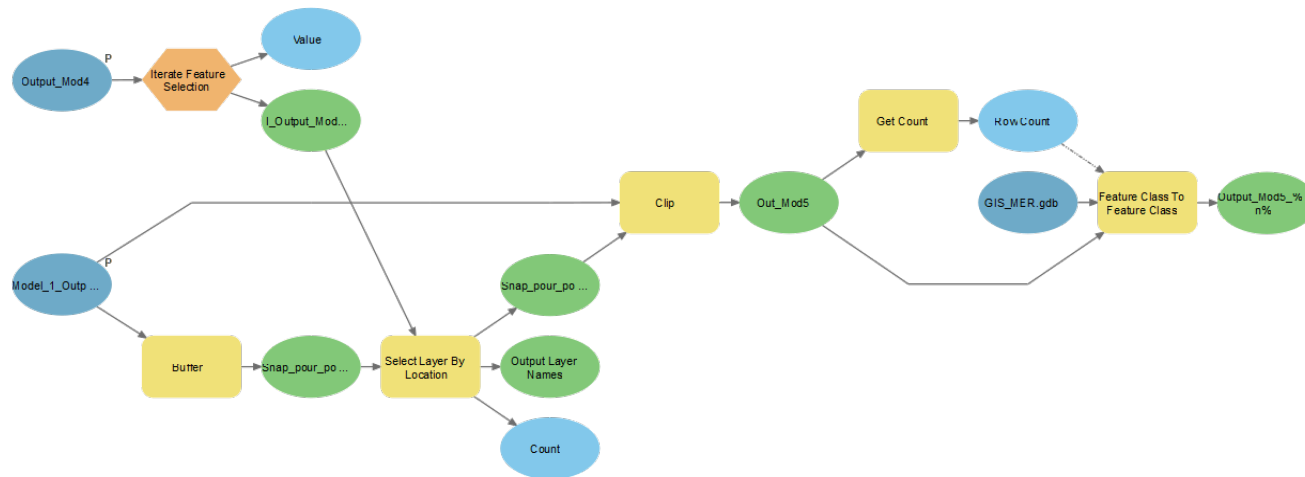


Figure A4. GIS-MER submodel 5 (iterate snap pour points selection and geoprocessing).

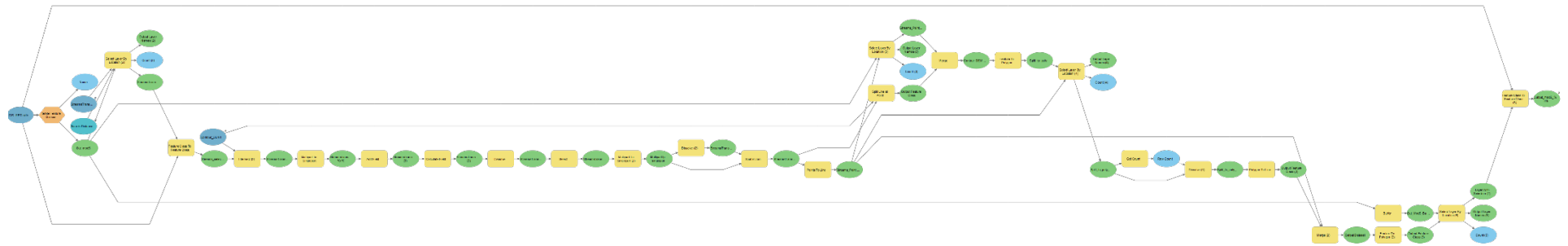


Figure A5. GIS-MER submodel 6 (iterate submodel 5—results geoprocessing).

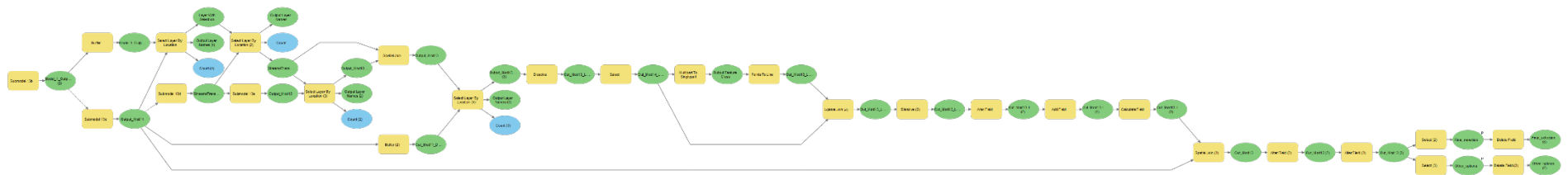


Figure A6. GIS-MER submodel 13 (geoprocessing, calculation and final results selection).

Appendix C

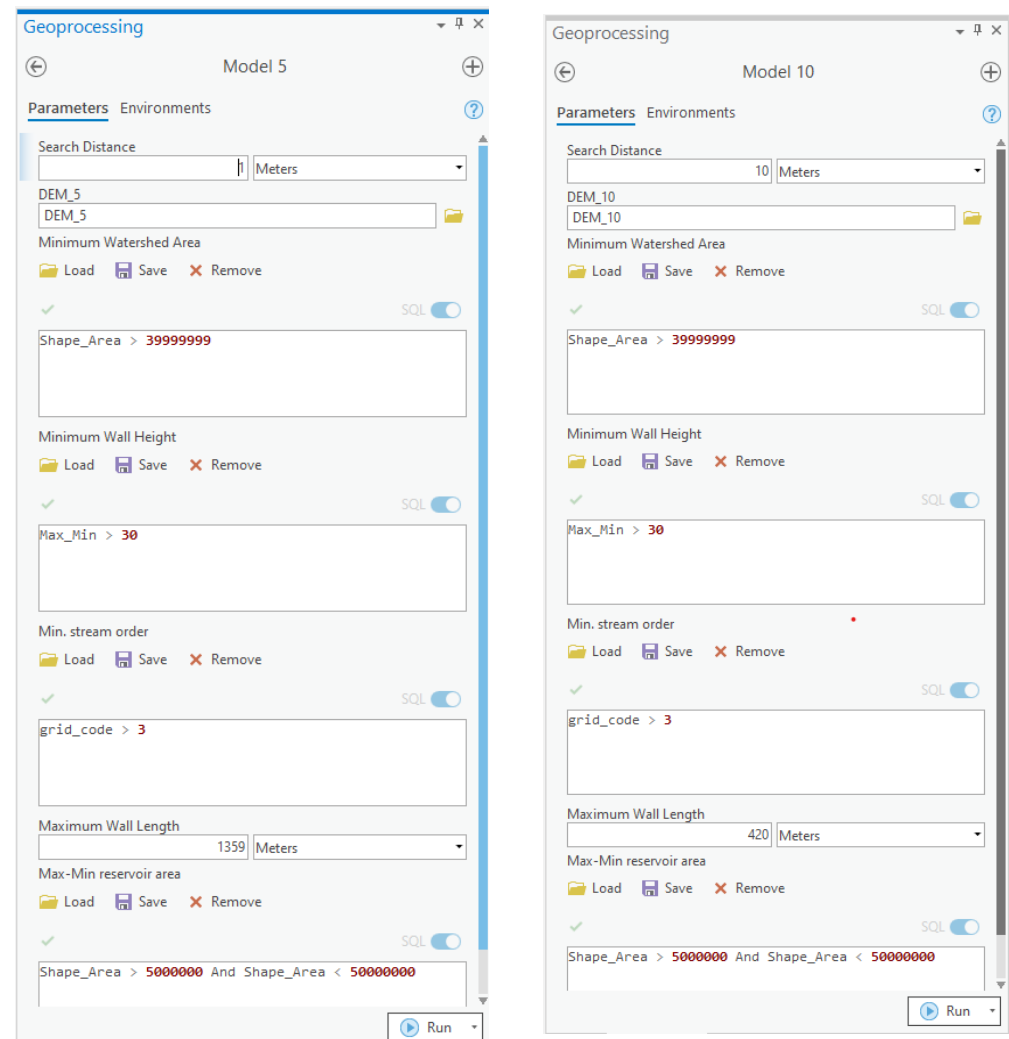


Figure A7. Model 5 and Model 10 interface in the ArcGIS Pro Geoprocessing panel.

References

1. Fader, M.; Shi, S.; von Bloh, W.; Bondeau, A.; Cramer, W. Mediterranean irrigation under climate change: More recent irrigation needed to compensate for increases in irrigation water requirements. *Hydrol. Earth Syst. Sci.* **2016**, *20*, 953–973. [\[CrossRef\]](#)
2. Kim, J.H.; Sung, J.H.; Shahid, S.; Chung, E.S. Future Hydrological Drought Analysis Considering Agricultural Water Withdrawal Under SSP Scenarios. *Water Resour. Manag.* **2022**, *36*, 2913–2930. [\[CrossRef\]](#)
3. Zarfl, C.; Lumsdon, A.E.; Berlekamp, J.; Tydecks, L.; Tockner, K. A global boom in hydropower dam construction. *Aquat. Sci.* **2015**, *77*, 161–170. [\[CrossRef\]](#)
4. Fischer, G.; Tubiello, F.N.; van Velthuizen, H.; Wiberg, D.A. Climate change impacts on irrigation water requirements: Effects of mitigation, 1990–2080. *Technol. Forecast. Soc. Chang.* **2007**, *74*, 1083–1107. [\[CrossRef\]](#)
5. Wang, Y.; Tian, Y.; Cao, Y. Dam Siting: A Review. *Water* **2021**, *13*, 2080. [\[CrossRef\]](#)
6. Martínez, V. Use of water resources in semi-arid areas. Evaporation in irrigation reservoirs and its possible solutions. In Proceedings of the Use and Management of Natural Resources in Semi-Arid Environments in the Mediterranean area: II International Mediterranean Conference, Mazarrón, Spain, 19–21 April 2013; 2014; pp. 133–142.
7. López Moreno, J.L. Estimation of water losses through evaporation in reservoirs in the Pyrenees. *Geogr. Res. Noteb.* **2008**, *34*, 61–81. [\[CrossRef\]](#)
8. Craig, I.; Green, A.; Scobie, M.; Schmidt, E. *Controlling Evaporation Loss from Water Storages*; Technical Report; University of Southern Queensland, National Centre for Engineering in Agriculture Publication 1000580/1; USQ: Toowoomba, Australia, 2005.
9. Friedrich, K.; Grossman, R.L.; Huntington, J.; Blanken, P.D.; Lenters, J.; Holman, K.D.; Gochis, D.; Livneh, B.; Prairie, J.; Skeie, E.; et al. Reservoir Evaporation in the Western United States: Current Science, Challenges, and Future Needs. *Bull. Am. Meteorol. Soc.* **2018**, *99*, 167–187. [\[CrossRef\]](#)

10. Rodrigues, C.M.; Moreira, M.; Cabral Guimarães, R.; Potes, M. Reservoir evaporation in a Mediterranean climate: Comparing direct methods in Alqueva Reservoir, Portugal. *Hydrol. Earth Syst. Sci.* **2020**, *24*, 5973–5984. [CrossRef]
11. Molina, J.M.; Álvarez, V.M.; Baille, A.; González-Real, M.M. Estimation of evaporation in irrigation reservoirs using an energy balance model. *Water Eng.* **2006**, *13*, 219–230.
12. Walsh, S.J.; Page, P.H.; McKnight, S.A.; Yao, X.; Morrissey, T.P. A reservoir siting tool for North Carolina: System design & operations for screening and evaluation. *Appl. Geogr.* **2015**, *60*, 139–149. [CrossRef]
13. Rahmati, O.; Kalantari, Z.; Samadi, M.; Uuemaa, E.; Davoudi, D.; Asadi, O.; Destouni, G.; Tien, B.D. GIS-Based Site Selection for Check Dams in Watersheds: Considering Geomorphometric and Topo-Hydrological Factors. *Sustainability* **2019**, *11*, 5639. [CrossRef]
14. Sayl, K.N.; Mohammed, A.S.; Ahmed, A.D. GIS-based approach for rainwater harvesting site selection. *IOP Conf. Ser. Mater. Sci. Eng.* **2020**, *737*, 012246. [CrossRef]
15. Mahmoud, S.H.; Tang, X. Monitoring prospective sites for rainwater harvesting and stormwater management in the United Kingdom using a GIS-based decision support system. *Environ. Earth Sci.* **2015**, *73*, 8621–8638. [CrossRef]
16. Rahman, N.F.A.; Awangku, A.A.H.; Tai, V.C.; Mohammad, M.; Haron, S.H.; Khalid, K.; Rasid, M.Z.A.; Shariff, S.M. Site selection of water reservoir based on weighted overlay in ArcGIS (case study: Bachok, Kelantan). *Sci. Int.* **2021**, *33*, 135–139.
17. Krois, J.; Schulte, A. GIS-based multi-criteria evaluation to identify potential sites for soil and water conservation techniques in the Ronquillo watershed, northern Peru. *Appl. Geogr.* **2014**, *51*, 131–142. [CrossRef]
18. Jozaghi, A.; Alizadeh, B.; Hatami, M.; Flood, I.; Khorrami, M.; Khodaei, N.; Ghasemi, E. A Comparative Study of the AHP and TOPSIS Techniques for Dam Site Selection Using GIS: A Case Study of Sistan and Baluchestan Province, Iran. *Geosciences* **2018**, *8*, 494. [CrossRef]
19. Al-Abadi, A.M.; Shahid, S.; Ghalib, H.B.; Handhal, A.M. A GIS-Based Integrated Fuzzy Logic and Analytic Hierarchy Process Model for Assessing Water-Harvesting Zones in Northeastern Maysan Governorate, Iraq. *Arab. J. Sci. Eng.* **2017**, *42*, 2487–2499. [CrossRef]
20. Othman, A.; Al-Maamar, A.F.; Ali Mohammed Amin Al-Manmi, D.; Liesenberg, V.; Hasan, S.E.; Obaid, A.K.; Fadhil Al-Quraishi, A. GIS-Based Modeling for Selection of Dam Sites in the Kurdistan Region, Iraq. *ISPRS Int. J. Geo-Inf.* **2020**, *9*, 244. [CrossRef]
21. Al-Ruzouq, R.; Shanableh, A.; Gokhan Yilmaz, A.; Idris, A.; Mukherjee, S.; Ali Khalil, M.; Barakat, A.; Gibril, M. Dam Site Suitability Mapping and Analysis Using an Integrated GIS and Machine Learning Approach. *Water* **2019**, *11*, 1880. [CrossRef]
22. Petheram, C.; Gallant, J.; Read, A. An automated and rapid method for identifying dam wall locations and estimating reservoir yield over large areas. *Environ. Model. Softw.* **2017**, *92*, 189–201. [CrossRef]
23. Wimmer, M.H.; Pfeifer, N.; Hollaus, M. Automatic Detection of Potential Dam Locations in Digital Terrain Models. *Isprs Int. J. Geo-Inf.* **2019**, *8*, 197. [CrossRef]
24. Teschemacher, S.; Bittner, D.; Disse, M. Automated Location Detection of Retention and Detention Basins for Water Management. *Water* **2020**, *12*, 1491. [CrossRef]
25. Instituto de Estadística y Cartografía de Andalucía. Available online: <https://www.juntadeandalucia.es/institutodeestadisticaycartografia/DERA/> (accessed on 11 September 2022).
26. Red de Información Ambiental de Andalucía. Available online: <https://www.juntadeandalucia.es/medioambiente/portal/acces-o-rediam> (accessed on 11 September 2022).
27. Portal Ambiental de Andalucía. Ámbito territorial y físico de la Demarcación Hidrográfica del Guadalete y Barbate. Available online: <https://www.juntadeandalucia.es/medioambiente/portal/areas-tematicas/agua/recursos-hidricos/demarcaciones-hidrograficas/ambito-territorial-y-fisico-de-la-demarcacion-hidrografica-del-guadalete-y-barbate> (accessed on 11 September 2022).
28. MITECO. Available online: <https://www.iagua.es/data/infraestructuras/presas> (accessed on 11 September 2022).
29. ESRI Dam Safety. Available online: <https://doc.arcgis.com/en/arcgis-solutions/latest/reference/introduction-to-dam-safety.htm> (accessed on 11 September 2022).
30. Suharyanto, S.; Harjanti, T.N.S.; Sriyana, I.; Suryadi, F. Location Suitability for Small Reservoirs at the Bodri-Kuto River Basin Based on Spatial Monthly SPI. *Water* **2020**, *12*, 993. [CrossRef]
31. Jensen, M.E. Estimating evaporation from water surfaces. In Proceedings of the CSU/ARS Evapotranspiration Workshop, Fort Collins, CO, USA, 15 March 2010.
32. Ledec, G.; Quintero, J.D. Good dams and bad dams: Environmental criteria for site selection of hydroelectric projects. Latin America and the Caribbean Region; In *Sustainable Development Working Paper*; World Bank: Washington, DC, USA, 2003; Volume 16, pp. 1–21.
33. Fleming, J.P.; Madsen, J.D.; Dibble, E.D. Development of a GIS model to enhance macrophyte re-establishment projects. *Appl. Geogr.* **2012**, *32*, 629–635. [CrossRef]
34. Wu, S.; Li, J.; Huang, G.H. A study on DEM-derived primary topographic attributes for hydrologic applications: Sensitivity to elevation data resolution. *Appl. Geogr.* **2008**, *28*, 210–223. [CrossRef]